Journal of ELECTRONIC MATERIALS, Vol. 46, No. 7, 2017
DOI: 10.1007/s11664-017-5436-6

Plasmonic Effect Enhanced Photocurrent in Nanostructured TiO_2 Films Decorated with Gold Nanoparticles

PHAM DUY LONG,[1,3] DANG TRAN CHIEN,[2] NGUYEN THANH TRUNG,[1] NGUYEN SI HIEU,[1] LE HA CHI,[1] VU VAN CAT,[1] and VU DINH LAM[1]

1.—Institute of Materials Science, Vietnam Academy of Science and Technology, 18 Hoang Quoc Viet Street, Hanoi, Vietnam. 2.—Hanoi University of Natural Resources and Environment, 18 Hoang Quoc Viet Street, Hanoi, Vietnam. 3.—e-mail: longphd@ims.vast.ac.vn

In this study we present the plasmonic effect enhanced photocurrent in gold (Au) decorated on nanostructured TiO_2 films (Au@TiO_2). The Au@TiO_2 electrodes were successfully prepared by means of vacuum evaporation, followed by thermal annealing. It was found that the average size of Au nanoparticles depends on the thickness of the deposited Au layer and the morphology of nanostructured TiO_2 films. Strong plasmonic resonance absorption effects were observed in the samples of Au deposited on TiO_2 nanoparticle films (Au@TiO_2-NPs) where the resonance absorption peaks shifted to red wavelengths ranging from 534 nm to 617 nm, when Au nanoparticles size changes from 14 nm to 65 nm. For the Au deposited on TiO_2 nanowire films (Au@TiO_2-NWs), we found that the resonance absorption peak with a large absorbance was located at 547 nm. Photovoltaic properties of the plasmonic solar cells based on Au@TiO_2 films as a working electrode were investigated. The results show that the enhancement in photocurrent caused by the plasmonic effect of the Au nanoparticles was strongly dependent on both their size and density.

Key words: Au@TiO_2 film, plasmonic effect, Au nanoparticles, TiO_2 Nanostructured film, vacuum evaporation

INTRODUCTION

Metallic nanoparticles coupling with semiconductor oxide nanoparticles have novel properties that are not found in the individual components.[1–4] The novel properties of these materials come from the formation of a surface plasmon resonance (SPR) effect at the interface of the semiconductor and the metal nanoparticle. It is well known that the nanostructure materials enhance the plasmon effect, which is caused by the collective oscillation of conductive electrons affected by the electric field of incident light.[5,6] Recently, Au@TiO_2 nanocomposite materials are the most studied for use in photocatalysis,[7–9] solar cells,[3,10–12] water splitting,[13] etc. This is because nanostructured TiO_2 (nc-TiO_2) can be easily prepared, and it possesses both the intensive photo-electrochemical property and the chemical stability. Moreover, nc-TiO_2 is non-toxic, thus it is friendly to the environment. Many studies have shown that the absorbance spectra of the plasmonic resonance of Au@TiO_2 nanocomposite materials are strongly dependent on the materials preparation parameters, such as the concentration, size, shape and behavior of Au nanoparticles.[14–17] Thus, by managing the preparation condition, one can enhance the absorbance of Au@TiO_2 resulting in improvement of the photocatalytic and photo-electrochemical properties of the materials. This is why Au@TiO_2 nanocomposites are very prospective in the field of research and manufacture of photocatalytic materials and solar cell devices with a large performance efficiency. In addition, the plasmonic effects of Au and Ag nanoparticles were also investigated to make so-called surface enhanced Raman spectroscopy (SERS) substrates. Numerous methods have been used to prepare Au@TiO_2 nanocomposite thin films,

(Received August 8, 2016; accepted March 2, 2017; published online March 17, 2017)

such as physics, chemical methods or their combination.[18–21] In our study, Au nanoparticles were dispersed onto TiO_2 nanostructure films by thermal evaporation of a very thin Au layer on the nanostructured TiO_2 films and then were annealed to form Au@TiO_2 nanocomposite films. As compared to other techniques, this simple method can produced a large area thin film with high uniformity, high purity, and good adhesion to substrates. The obtained results have shown that the Au nanoparticles are uniformly dispersed on the nanostructured TiO_2 films and their size was dependent on the thickness of the Au-deposited layer and morphology of TiO_2 nanostructure films. From the absorption properties study, it is seen that Au@TiO_2 nanocomposite materials exhibited good SPR absorption effects and their SPR absorption peak changes in the range of 530 nm to 620 nm depending on particle size or thickness of deposited Au film. The photovoltaic properties of plasmonic solar cells based on Au@TiO_2 films have been investigated. The results showed that due to the SPR effect of Au nanoparticles deposited on nc-TiO_2 films, the photocurrent of the devices is considerably enhanced, and the photocurrent enhancement depended on both the size and density of the gold nanoparticles.

EXPERIMENTAL

Gold nanoparticles decorated on nc-TiO_2 films (Au@TiO_2) were prepared by vacuum evaporation. The thin Au layers deposited on the nc-TiO_2 films have different surface morphology. In our studies, we used three types of samples for characterization as follows: the TiO_2-nanoparticle films were grown on single glass substrates (further abbreviated to glass/TiO_2-NPs), on FTO-coated glass (FTO/TiO_2–NPs) and TiO_2-nanowire films grown on FTO-coated glass (FTO/TiO_2-NWs). The TiO_2-NPs films were fabricated by Dc-sputtering of 100 nm thick titanium layers on the glass and glass/FTO substrates and then annealed at 450°C for 4 h in air. The detailed preparation process can be seen elsewhere.[22] The TiO_2-NWs films were obtained by hydrothermal treatment of the sputtered titanium films in a 5 M NaOH solution at 90°C for 2 h as mentioned in Ref. 23. The samples were then annealed at 450°C for 1 h. All the nanostructured TiO_2 films were loaded into a vacuum chamber to conduct the Au layer deposition by the thermal evaporation method. The depositing process was conducted at a pressure of 1.33×10^{-6} kPa on the unheated substrates. The thickness of the Au layer was monitored and controlled by using a quartz microbalance. In this study, Au layers with three different thicknesses (namely 3.0 nm, 4.5 nm, and 8.0 nm) were deposited. Then the samples were annealed at 400°C for 2 h in air to form Au@TiO_2 nanocomposite films. The surface morphology of the nanocomposite films was studied by using a Hitachi field emission scanning electron microscope (FE-SEM). The absorption spectra of the films were recorded using a Shimadzu UV-1800 spectrometer. To characterize performance parameters of solar cells, devices in the configuration of FTO/Au@TiO_2/(I^-/I^{3-})electrolyte/Pt were prepared. Their photocurrent − voltage (I/V) characteristics were recorded by using a Keithley 2400 source meter under irradiation of a 150 W xenon lamp equipped with an AM 1.5G filter (Newport) with light intensity adjusted to 1-Sun condition (100 mW/cm^2).

RESULTS AND DISCUSSION

Figure 1 shows the FE-SEM images of Au@TiO_2 films obtained from the evaporation of a 4.5 nm thick Au layer on the FTO/TiO_2-NPs films in which Fig. 1a is a FE-SEM image of as-deposited films; Fig. 1b is the image of the annealed one. From these images one can see that the Au layer in as-deposited film exhibited a smooth layer covered onto the surface of the nc-TiO_2 film. When the films were annealed, the Au atoms had a tendency to concentrate to form Au nanoparticles, and these nanoparticles dispersed well on the nc-TiO_2 film. The average size of Au nanoparticles of about 22 nm in diameter was determined as shown in the diagram in Fig. 1c. This proves that Au@TiO_2 nanocomposite films were successfully fabricated by a simple vacuum evaporation method.

We investigated the effect of the gold layer thickness as well as the morphology of nc-TiO_2 substrates on both the formation and Au nanoparticles size by using FE-SEM images. Figure 2

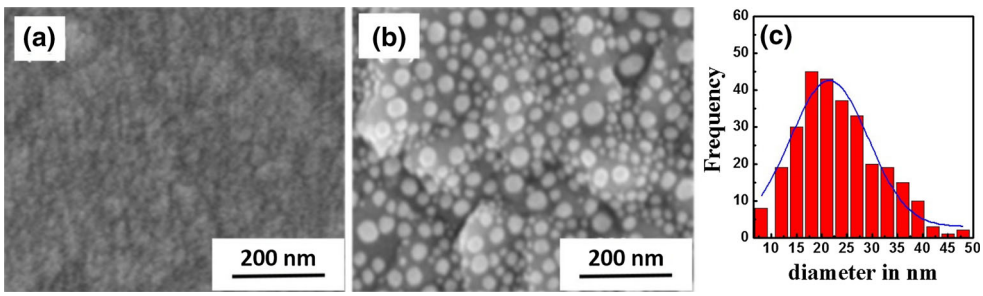

Fig. 1. FE-SEM image of Au@TiO_2 films prepared by evaporation of a 4.5 nm thick Au layer on nc-TiO_2 films. (a) as-deposited film; (b) after annealed at 400°C for 2 h and (c) the grain size distribution with Gauss fitting for the annealed sample.

presents FE-SEM images of Au@TiO_2 nanocomposite films prepared with different values of the Au layer thickness (namely 3.0 nm, 4.5 nm, and 8.0 nm) using nc-TiO_2 substrates of different surface morphology as mention in the experimental section. Those are the FE-SEM images of the Au nanoparticles deposited on glass (Fig. 2a, b, and c corresponding to the Au layer thickness d = 3.0 nm, 4.5 nm, and 8.0 nm); on TiO_2-NPs coated glass (Fig. 2d, e, and f); on TiO_2-NPs coated FTO (FTO/Au@TiO_2-NPs) see Fig. 2g, h, and i. Finally, FE-SEM images of the Au nanoparticles deposited on FTO/TiO_2-NWs substrates (FTO/Au@TiO_2-NWs) are shown in Fig. 2j, k, and l.

From these FE-SEM images, one can note that the size of Au nanoparticles increased with the increase of the Au layer for all Au@TiO_2-NPs samples. The average sizes of Au nanoparticles

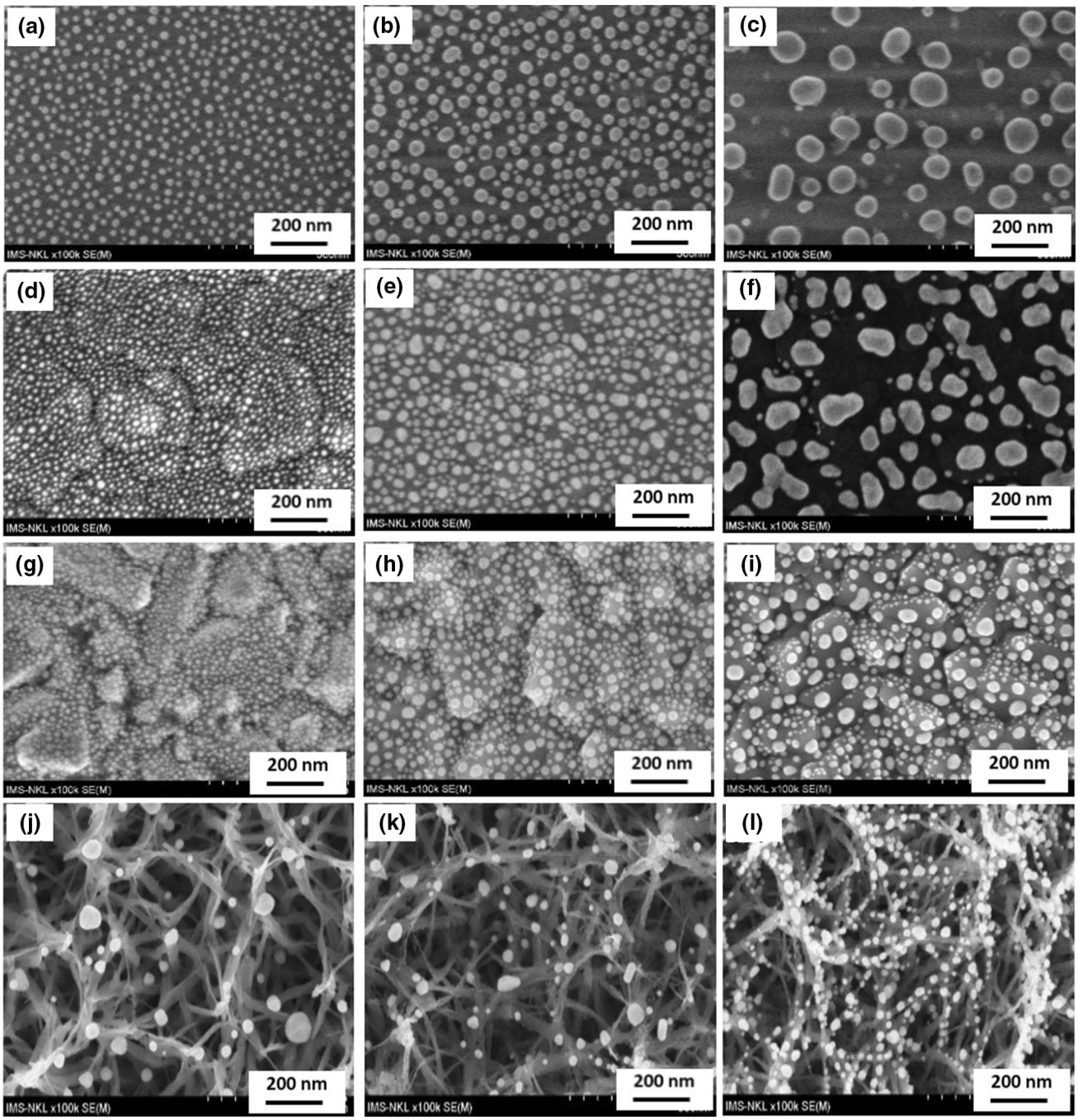

Fig. 2. FE-SEM images of Au@TiO_2 nanocomposite films with three different Au layer thicknesses (d = 3.0 nm, 4.5 nm, and 8.0 nm) deposited on different substrates: (a–c) on glass substrates; (d–f) on glass/TiO_2-NPs substrates; (g–i) on FTO/TiO_2-NPs substrates and (j–l) on FTO/TiO_2-NWs substrates.

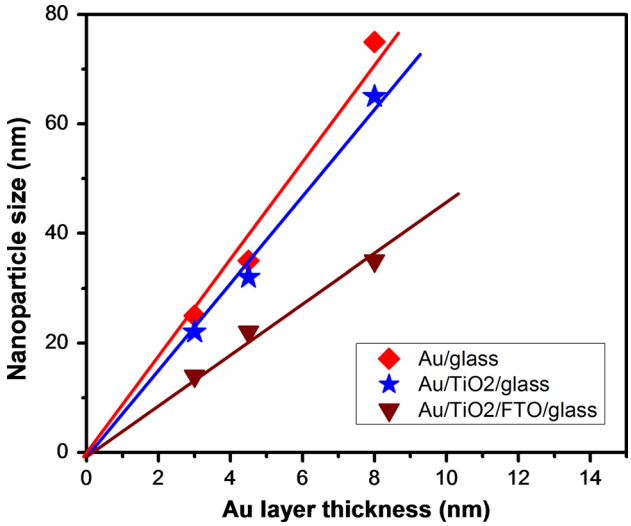

Fig. 3. The dependence of Au nanoparticle size on the thickness of evaporated Au layers.

deposited on glass substrates were of 25 nm, 35 nm, and 75 nm that correspond to d = 3.0 nm, 4.5 nm, and 8.0 nm. These sizes were slightly larger than those of Au nanoparticles grown on glass/TiO_2 NPs substrates (namely 22 nm, 32 nm, and 65 nm) and on FTO/TiO_2-NPs substrates (namely 14 nm, 22 nm, and 35 nm). Whereas, using FTO/TiO_2-NWs substrates, the size of Au nanoparticles seems to be unchanged with the increase in the Au layer thickness, and their size was kept at a value of ca. 22 nm. However, we observed the significant increase of the density of the gold nanoparticles with thicker Au layer (see Fig. 2j, k, and l). The size and density of Au nanoparticles depended on the Au layer thickness and surface morphology of nc-TiO_2 substrates as shown in Table I. This clearly shows the substrate morphology effect on the Au nanoparticle size. Indeed, the surface roughness of the four kinds of substrates increased from glass to glass/TiO_2-NPs and FTO/TiO_2-NPs. Especially, in FTO/TiO_2-NWs substrates we observed are not only rough but also a very porous surface (Fig. 2). This is the reason why Au nanoparticles grown on these substrates possess a smaller size and a higher density.

Figure 3 presents the diagram of the dependence of Au nanoparticle size on the thickness of the Au layer deposited on different substrates as mentioned above. The diagram indicated that the Au nanoparticle sizes are raised almost linearly with the Au layer thickness. Moreover, the slope of lines is inversely proportional to the roughness of substrate surfaces at the same value of thickness of the Au layers deposited. The rougher the substrate surface, the smaller the Au nanoparticles that were grown.

The plasmonic effects of Au@TiO_2 nanocomposite films were revealed through the absorption spectra in the visible light region of the films. Figure 4 shows the absorption spectra of all the abovementioned Au@TiO_2 nanocomposite films. From the spectra, it is clearly seen that the plasmonic resonance absorption effects were observed in all samples. The SPR absorption peaks of Au nanoparticles deposited on glass, glass/TiO_2-NPs and FTO/TiO_2-NPs substrates were shifted to the red wavelength range, when either the thickness of Au layer or the size of the Au nanoparticles increased. The peak positions shifted from 530 nm to 620 nm with Au layer thickness changing from 3.0 nm to 8.0 nm, as can be seen in Fig. 4. We also found that the full width at half maximum (FWHM) of SPR absorption peaks increased with the increase of the substrate roughness from glass to glass/TiO_2-NPs and FTO/TiO_2-NPs. It is observed that the better uniform Au nanoparticles were grown on the less rough substrate surface. In the case of Au nanoparticles deposited on FTO/TiO_2-NWs substrates, the SPR absorption peak position remained at 547 nm even when the Au layer thickness significantly changed. However, the intensity of the absorption peaks significantly increased in the samples with the thicker Au layer. This can be explained because of the increase of the density of the Au nanoparticles of 20 ÷ 25 nm in size in the samples deposited on FTO/TiO_2-NWs substrates as shown in the FE-SEM images (see Fig. 2j, k, and l) and in Table I.

Finally, we used FTO/Au@TiO_2-NPs and FTO/AuTiO_2-NWs films as photoactive materials for preparing plasmonic solar cells, abbreviated to PPSC and WPSC, respectively. The PPSC and WPSC devices have a configuration of FTO/Au@TiO_2-NPs/(I^-/I^{3-})Electrolyte/Pt and FTO/Au@TiO_2-NWs/(I^-/I^{3-})Electrolyte/Pt, respectively. Photovoltaic properties of the cells were investigated by recording their photocurrent–voltage (I/V) characteristics under 1.5 M irradiation condition; the obtained results are shown in Fig. 5. From the figure one can see that both short-circuit current density (J_{sc}) and open-circuit voltage (V_{oc}) of the cells were significantly enhanced compared to the solar cells made from pure nc-TiO_2 electrodes. For the PPSC, there was a nonlinear dependence of the J_{sc} on the size of Au nanoparticles, and the largest photocurrent was obtained on the samples with Au layer thickness d = 4.5 nm and/or with Au particle size of 22 nm, whereas V_{oc} increased in the devices with larger Au nanoparticles. The enhancement of the J_{sc} and V_{oc} can be explained by the transfer of hot electrons generated by the SPR effect from Au nanoparticles to the conduction band of nc-TiO_2 materials. As we know, the number of electrons can transfer from Au nanoparticles to TiO_2 materials depending on energy of hot electrons that corresponds to the energy of excitation light in the SPR absorbance and the interface area of Au nanoparticle with TiO_2 materials. When Au nanoparticle size is small, almost all of the hot electrons can overcome the Shottky barrier formed at the contact layer of

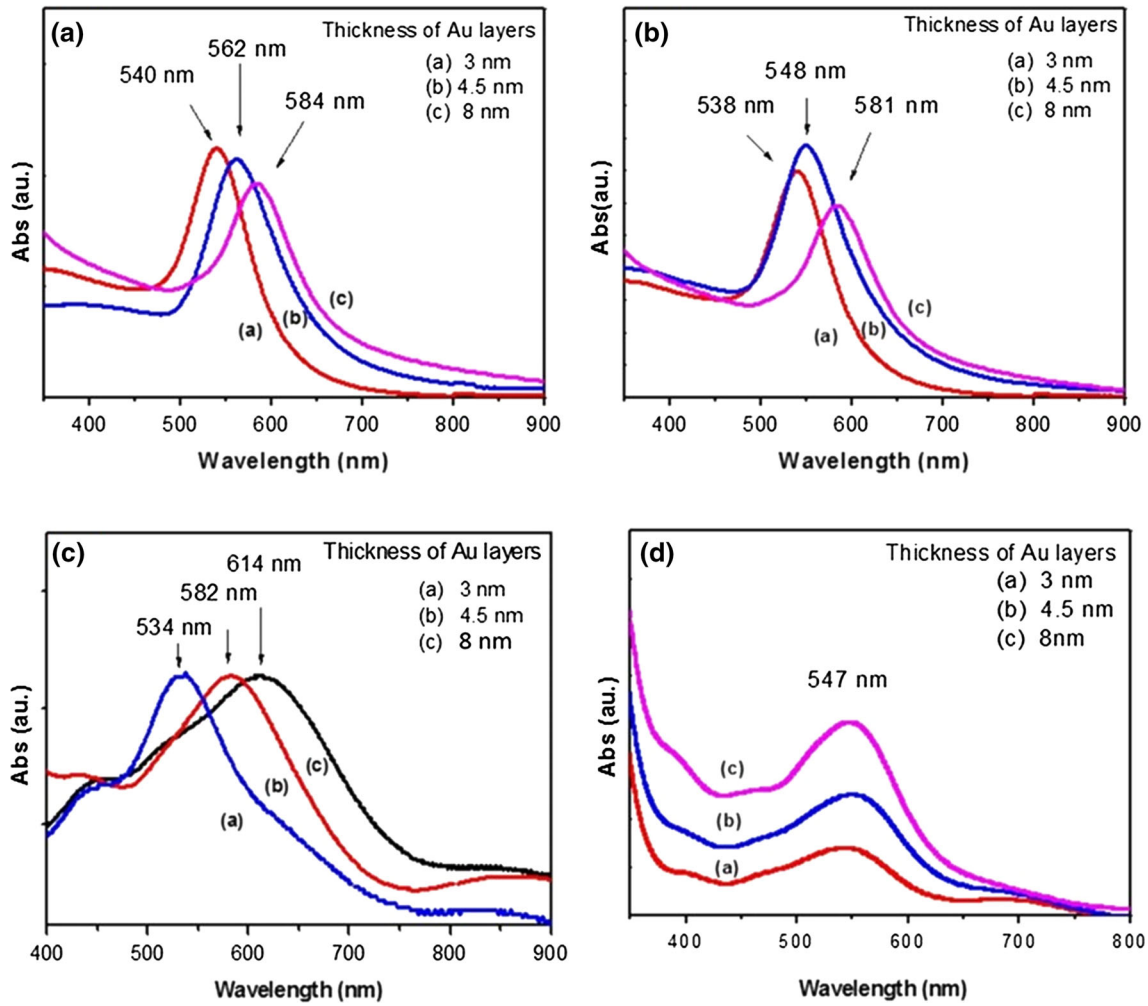

Fig. 4. Absorption spectra of$Au@TiO_2$ nanocomposite films with different Au layer thicknesses (d = 3.0 nm, 4.5 nm, and 8.0 nm) deposited on different substrates. (a) on glass substrates; (b) on glass/TiO2-NPs; (c) on FTO/TiO_2-NPs substrates and (d) on FTO/TiO_2-NWs substrates.

Table I. The size and density of Au nanoparticles of Au@TiO_2 films versus Au layer thickness

Au layer thickness		**3.0 nm**	**4.5 nm**	**8.0 nm**
Glass sub.	Average particle size (nm)	25	35	75
	Density (Number of particles/μm^2)	710	364	59
Glass/TiO_2-NPs sub.	Average particle size (nm)	22	32	65
	Density (Number of particles/μm^2)	2517	614	87
FTO/TiO_2-NPs sub.	Average particle size (nm)	14	22	35
	Density (Number of particles/μm^2)	2106	835	647
FTO/TiO_2-NWs sub.	Average particle size (nm)	25	20	22
	Density (Number of particles/μm^2)	61	101	529

gold and TiO_2 materials. Thus, the density of electrons in the conduction band of nc-TiO_2 increased and caused the rise of the effective Fermi level of the nanocomposite system. This is related to the increase of J_{sc} and V_{oc}. When the Au nanoparticle size is too large, the excited energetic level of hot electrons decreased due to the shift of the SPR peak to lower energy, then the number of electrons injected into the conduction band of nc-TiO_2 materials became lower. Then electrons in Au nanoparticles were accumulated due to the Fermi level of gold being lower than the conductive band of nc-TiO_2. This causes the rise of the Fermi level in gold materials and then the effective Fermi level as predicted in Ref. 24. These are the reasons that make the J_{sc} become smaller but V_{oc} is larger compared to that value of smaller Au nanoparticles as seen in Fig. 5a.

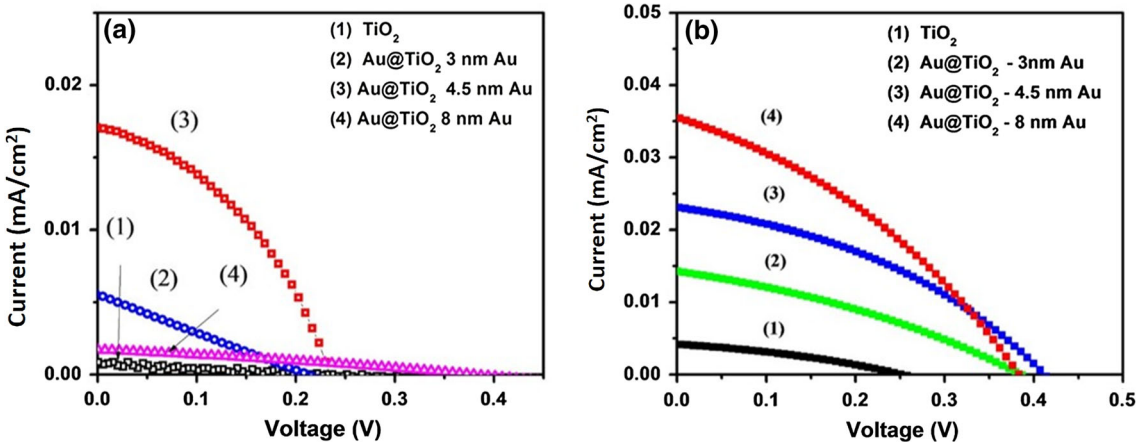

Fig. 5. I/V characteristics of solar cells based on Au@TiO_2 films as photo-anodes irradiated in condition of AM 1.5. (a) For PPSC devices based on FTO/Au@TiO_2-NPs electrodes with different Au layer thicknesses; (b) for WPSC devices based on FTO/Au@TiO_2 NWs electrodes with different Au layer thicknesses.

In the case of WPSCs, the increase of the Au thickness layer made Au nanoparticles density increase, consequently, the photocurrent significantly increased too (see Fig. 5b). This can be explained by the enhancement of the light harvesting in the visible range caused by plasmonic effects in the Au@TiO_2-NWs films, when thicker Au layers were deposited (as shown in Fig. 4). For the WPSCs made from a 8.0 nm thick Au layer, J_{sc} reached a value as large as 0.035 mA/cm^2 that is ten times larger than that (0.0034 mA/cm^2) of the cells made from pure nc-TiO_2 electrodes. In addition, V_{oc} of the WPSCs is also much enhanced, namely, V_{oc} = 0.38 V compared to V_{oc} = 0.24 V (for the pure nc-TiO_2 solar cells). In this case, the change of V_{oc} was related to the change in density of the Au nanoparticle in Au@TiO_2 films in which the density increased with increasing Au layer thickness as presented in Table I. The dependence of V_{oc} on thickness of the Au layer or the density of Au nanoparticles can be explained as follows: First of all, the increasing density of the Au nanoparticle means that more electrons can be injected into the TiO_2 nanowire conductive band, making both J_{sc} and V_{oc} increase. However, the increasing concentration of electrons in TiO_2-NWs can make the combination processes of the electrons from the TiO_2-NWs conductive band with anions (I^{3-}) in electrolyte solution rise when the V_{oc} decreased. That is why V_{oc} of the device based on Au@TiO_2-NWs films of 8.0 nm thick Au layer-based solar cells is smaller than that of a device with 4.5 nm thick Au layer as shown in Fig. 5b.

CONCLUSIONS

Gold nanoparticles dispersed on the TiO_2 nanostructure films were successfully prepared by evaporation of a Au thin layer, followed by thermal annealing. The size and density of Au nanoparticles was found to be dependent on the thickness of the evaporated thin Au layer as well as on the morphology of TiO_2 nanostructure films. For the Au@TiO_2-NPs films with the smooth nc-TiO_2 films surface, the size of Au nanoparticles increased from 14 nm to 65 nm almost linearly with the evaporated Au layer thickness increasing from 3.0 nm to 8.0 nm. Strong plasmonic resonance absorption effects were observed in Au@TiO_2-NPs samples where the SPR peaks shifted from 534 nm to 614 nm, corresponding to the Au nanoparticle size changing from 14 nm to 65 nm. For the Au@TiO_2-NWs samples, only the density of Au nanoparticles increased with increasing Au layer thickness while their size remained at about 22 nm. The resonance absorption peak was located at 547 nm with a considerably large absorbance in the thicker gold layers. The investigations on the photovoltaic properties of solar cells based on Au@TiO_2 films serving as working electrodes indicated that, due to the plasmonic effect of gold nanoparticles, both the short-circuit current density and the open-circuit voltage of the solar cells were much enhanced. The photocurrent nonlinearly depended on the size of Au nanoparticles, and the strongest effect was obtained with their size around 22 nm. Besides, the photocurrent increased with the increase of Au nanoparticle density. For the devices made from Au@TiO_2-NWs (WPSC) film with a 8.0 nm thick Au layer, J_{sc} reached a value as large as 0.035 mA/cm^2 that is about ten times larger than that of the devices made from pure nc-TiO_2 electrodes. V_{oc} of the WPSCs was found to be of ca. 0.38 V that is much larger than (0.24 V) of the pure nc-TiO_2 solar cells.

ACKNOWLEDGEMENTS

This work was supported in part by the Science and Technology Research Projects of the Vietnam Academy of Science and Technology, the project

code: VAST03.05/13-14. A part of the work was done with the help of the Key Laboratory in Electronic Materials and Devices, Institute of Materials Science, Vietnam Academy of Science and Technology. We would like to thank the colleagues for their contribution to the work.

REFERENCES

1. X. Li, J. Fu, M. Steinhart, D.H. Kim, and W. Knoll, *Bull. Korean Chem. Soc.* 28, 1015 (2007).
2. F. Han, V. Kambala, M. Srinivasan, D. Rajarathnam, and R. Naidu, *Appl. Catal. A Gen.* 359, 25 (2009).
3. W.-C. Tu, Y.-T. Chang, H.-P. Wang, C.-H. Yang, C.-T. Huang, J.-H. He, and S.-C. Lee, *Sol. Energ. Mater. Sol.* 101, 200 (2012).
4. X. Jinxia, X. Xiangheng, S. Andrey, R. Fen, W. Wei, C. Guangxu, Z. Shaofeng, D. Zhigao, M. Fei, and J. Changzhong, *Nanoscale Res. Lett.* 8, 73 (2013).
5. L. Du, A. Furube, K. Hara, R. Katoh, and M. Tachiya, *Proc. SPIE* 6831, 68310W-1 (2007).
6. N. Van Hieu and N. Bich Ha, *Adv. Nat. Sci: Nanosci. Nanotechnol.* 5, 035004 (2014).
7. B. Min, J. Heo, N. Youn, O. Joo, H. Lee, J. Kim, and H. Kim, *Catal. Commun.* 10, 712 (2009).
8. D. Wang, Y. Zou, S. Wen, and D. Fan, *Appl. Phys. Lett.* 95, 012106 (2009).
9. B.H. Nguyen, V.H. Nguyen, and D.L. Vu, *Adv. Nat. Sci: Nanosci. Nanotechnol.* 6, 033001 (2015).
10. L. Qiao, D. Wang, L. Zuo, Y. Ye, J. Qian, H. Chen, and S. He, *Appl. Energy* 88, 848 (2011).
11. B.H. Nguyen and V.H. Nguyen, *Adv. Nat. Sci: Nanosci. Nanotechnol.* 6, 043001 (2015).
12. T. Hong Nhung, N. Van Hieu, N. Bich Ha, and V. Dinh Lam, *Adv. Nat. Sci. Nanosci. Nanotechnol.* 7, 013001 (2016).
13. J. Lee, S. Mubeen, X. Ji, G.D. Stucky, and M. Moskovits, *Nano Lett.* 12, 5014 (2012).
14. E. Hutter and J.H. Fendler, *Adv. Mater.* 16, 1685 (2004).
15. S. Pillai and M.A. Green, *Sol. Energ. Mater. Sol.* 94, 1481 (2010).
16. Z. Li, S. Butun, and K. Aydin, *ACS Photon.* 1, 228 (2014).
17. L.V. Hong, D.T. Cat, L.H. Chi, N.T. Thuy, T.V. Hung, L.N. Tai, and P.D. Long, *Elecron. Mater.* 45, 4833 (2016).
18. A. Ito, H. Masumoto, and T. Goto, *Mater. Trans.* 44, 1599 (2003).
19. Y. Tian and T. Tatsuma, *J. Am. Chem. Soc.* 127, 7632 (2005).
20. N. Suratun, O. Arfian, U. Akrajas Ali, S. Muhammad Mat, B. Aamna, and S. Siti Khatijah Md, *J. Phys. Conf. Ser.* 431, 012011 (2013).
21. N. Van-Quynh, S. Delphine, M. Pascal, and L. Jean-Christophe, *Adv. Nat. Sci: Nanosci. Nanotechnol.* 7, 015005 (2016).
22. D.T. Chien, P.D. Long, L.H. Chi, and P.V. Hoi, *Adv. Nat. Sci: Nanosci. Nanotechnol.* 1, 015002 (2010).
23. J.-Z. Chen, W.-Y. Ko, Y.-C. Yen, P.-H. Chen, and K.-J. Lin, *ACS Nano* 6, 6633 (2012).
24. V. Subramanian, E.E. Wolf, and P.V. Kamat, *J. Am. Chem. Soc.* 126, 4943 (2004).